International Journal of Pharmaceutics 422 (2012) 185–193

Contents lists available at SciVerse ScienceDirect

International Journal of Pharmaceutics

journal homepage: www.elsevier.com/locate/ijpharm

Polymorphic and kinetic investigation of adefovir dipivoxil during phase transformation

Ji-Hun An[a], Guang Jin Choi[b], Woo-Sik Kim[a,*]

[a] Department of Chemical Engineering, ILRI, Kyunghee University, Kyungki-do 449-701, Republic of Korea
[b] Department of Pharmaceutical Engineering, Inje University, Gimhae, Gyeongnam 621-749, Republic of Korea

ARTICLE INFO

Article history:
Received 19 July 2011
Received in revised form 24 October 2011
Accepted 27 October 2011
Available online 4 November 2011

Keywords:
Polymorphic transformation
Polymorph search
Kinetics
Nucleation model
Mass transfer

ABSTRACT

To search polymorphs of adefovir dipivoxil (AD), the polymorphic transformation approach in solution was developed. Also, the kinetics of polymorphic transformation was investigated to effectively control polymorphs. The AD crystals were obtained by crystallization at −10 °C, and then the polymorphic transformation was induced by raising temperature. The polymorphs of AD were confirmed using DSC, XRD and solubility analyses. The polymorphic fraction during transformation was monitored for kinetic investigation. Via polymorphic transformation in solution, four polymorphs of AD were found and two of them were new (NF-I, NF-II). The DSC analysis revealed that solvate form (NF-I) was changed to form-V in solid state, and then re-crystallized to NF-II at 93 °C, and finally became form-I at 97 °C. This serial change of polymorphs in DSC was identical to polymorphic transformation sequence in solution. The kinetic rates of polymorphic transformation described by nucleation and mass transfer theories were well matched with experimental measurement. The polymorphic transformation approach was effective to search polymorphs of which the structure was changed to the other one in the solution. The kinetic information of polymorphic transformation predicted by Volmer's nucleation model and Stokes–Einstein diffusion equation was valuable for exact control of polymorphic purity.

1. Introduction

In pharmaceutics, polymorphism is one of the most important factors in the production of active pharmaceutical ingredient (API) crystals, as the physicochemical properties of API crystals, such as their solubility, structural stability, dissolution rate, density, and melting point, are all directly dictated by the class of the polymorph (Bernstein, 2002; Hilfiker, 2006; Purohit and Venugopalan, 2009; Sarma et al., 2011). Thus, polymorphic screening and phase transformation by API crystallization have attracted a great deal of attention for drug development, as the polymorph of API crystals determines the processability and bioavailability of a drug, and its shelf life.

The polymorphs of APIs are based on different 3-dimensional packing arrangements of the same molecules in a solid state resulting from different interactions between the molecules usually induced by the thermodynamic variables of the crystallization, such as the solvent, supersaturation, temperature, and additives. Thus, the thermodynamic conditions are invariably used for the investigation of polymorphs. In a diflunisal (Martinez-Oharriz et al., 1994), a polar solvent of methanol and ethanol produces different polymorphic crystals (form-III) from those (forms-I and IV) obtained with a non-polar solvent of toluene, chloroform, and carbon tetrachloride, as different hydrogen interactions between the pharmaceutical molecules are induced by the different polarities of the solvents. Similarly, polymorphism depending on the solvent has also been observed in the crystallization of dipyridodiazeoinone and erythromycin (Mirza et al., 2003; Pereira et al., 2007). Meanwhile, the influence of the supersaturation on polymorphs has been clearly demonstrated in the crystallization of 2-(3cyano-4-(2-methylpropoxy) phenyl)-4-methylthiazole-5-carboxylate (BPT ester) (Kitamura et al., 2006; Kitamura and Hara, 2007) where stable crystals are favorably generated at a low supersaturation, whereas metastable crystals are obtained at a high supersaturation.

Sometimes, conformational polymorphism has been encountered in crystallization due to the conformational deformation of pharmaceutical molecules by a solvent, as demonstrated by the crystallization of taltirerin (Maruyama and Ooshima, 2000). Here, the dihydromethylorotic acid and prolonamido moiety of the taltirerin in the water–methanol solution were conformationally rotated and the degree of the rotation depended on the composition of the water and methanol, resulting in two distinctive conformational α- and β-form polymorphs in the crystals.

* Corresponding author. Current address: School of Chemical Engineering and Biomolecular Engineering, Cornell University, Ithaca, NY 14853-5210, USA.
Tel.: +82 31 201 2576; fax: +82 31 273 2971.
E-mail address: wskim@khu.ac.kr (W.-S. Kim).

0378-5173/$ – see front matter © 2011 Elsevier B.V. All rights reserved.
doi:10.1016/j.ijpharm.2011.10.049

Such conformational polymorphs have also been observed in the pharmaceutical crystals of eflucimibe, ROY, enalapril maleate, and stavudine (Bernstein, 2002; Kiang et al., 2003; Mirmehrabi and Rohani, 2006; Smith et al., 2006; Purohit and Venugopalan, 2009; Lu and Rohani, 2009). In case of ROY, the molecular conformation is generated by the rotation of the aromatic ring, resulting in ten kinds of polymorph exhibiting different colors (Smith et al., 2006; Purohit and Venugopalan, 2009). The conformational polymorphs of stavudine also originate from the orientation of the aromatic ring of the molecule (Mirmehrabi and Rohani, 2006; Lu and Rohani, 2009), which depends on the supersaturation level and solvent. Using a molecular simulation, Kiang et al. (2003) demonstrated that the polymorphism of enalapril maleate was due to the rotation of the phenyl ring and methyl group of the molecule.

An ionic liquid can also be used for polymorph investigation as it induces a unique interaction between molecules, as distinct from conventional organic solvents. However, surprisingly, few studies have explored the use of ionic liquids for investigating polymorphs. One study used $AEImBF_4$ as a solvent for investigating the polymorphs of adefovir dipivoxil (AD) in drowning-out crystallization (An et al., 2010). In this case, the ionic liquid had a thermally stabilizing effect on the AD molecules, which were then easily decomposed in a conventional methanol–water mixture at temperatures above 30 °C. As a result of this thermal effect of $AEImBF_4$, a new anhydrate polymorph of AD was achieved at a high temperature above 90 °C. An ionic liquid ($BMImBF_4$) was also applied to the protein crystallization of lysozyme in order to vary its crystal structure. As a result, the surface charge distribution of the lysozyme protein was altered by the strong variability of the ionic shape of $BMImBF_4$, producing crystals with different structures to those produced with conventional salt ions.

In contrast to polymorphism that occurs in a solid state at equilibrium, phase transformation is spontaneous and dynamic behavior that occurs in a transient state, depending on the chemical potential difference. Thus, understanding the dynamics of phase transformation is important for the effective production of crystals of a target polymorph (Doremus, 1985; Chemburkar et al., 2000; Davey and Cardew, 1986). Therefore, various studies have already explored phase transformation in terms of the thermodynamic factors, such as the solvent, temperature, and additives (Sato et al., 1985; Qu et al., 2006, 2007, 2011) plus the kinetic factors, such as the supersaturation, solution viscosity, agitation, seeding, and seed size (Sato et al., 1985; Liang et al., 2004; Qu et al., 2006, 2007, 2011).

For example, Qu et al. (2006) studied the transformation of carbamazepine (CBZ) when varying the temperature. Here, the temperature was found to promote nucleation and mass transfer by reducing the energy barriers, while simultaneously reducing the supersaturation level that also influenced the nucleation and mass transfer rates. Thus, the phase transformation was enhanced when the effect of the temperature on reducing the energy barriers for nucleation and mass transfer surpassed its effect on reducing the supersaturation level, whereas the phase transformation was retarded when the effect of the temperature reduced the supersaturation more than the energy barriers. Similar results have also been observed in the phase transformation of piroxicam (Qu et al., 2011). Meanwhile, in the case of silfamerazine (SMZ), the composition of the solvent was shown to be a critical factor in determining the phase transformation, as it significantly changed the solubility of the polymorphs (Gu and Grant, 2001). In addition, Kurotani and Hirasawa (2008) applied ultrasound to promote the phase transformation of SMZ, thereby reducing the induction time of form-II SMZ. Furthermore, for o-aminobenzoic acid, the polymorphic pathway of the phase transformation was found to depend on the temperature, as form-II and form-II crystals were transformed to form-I crystals below a temperature of 50 °C. However, above 60 °C, the polymorphic pathway was changed to form-I → form-II → form-III due to an enantiotropic system of polymorphs depending on the temperature.

Consequently, as described above, phase transformation can temporarily facilitate the formation of specific polymorphs, indicating the potential importance of phase transformation to polymorph investigation. However, this area has not yet been systematically explored. Accordingly, the present study investigated the polymorphic transformation of AD crystals in terms of temperature as the primary factor influencing their polymorphism and phase transformation. In addition, the kinetics of the polymorphic transformation were also investigated as regards the induction and re-construction times, which is valuable information when designing a crystallization process for the precise production of a target polymorph. The crystal polymorphs were confirmed using XRD, DSC, TGA, and solubility analyses.

2. Materials and methods

2.1. Materials

The adefovir dipivoxil (AD; purity higher than 99.9%) was supplied from a Korean Pharmaceutical Company (Daehee Chem. Co., Korea) and used without further purification, while the solvent (dichloromethane (DCM), purity higher than 99.5%) and anti-solvent (n-hexane, purity 99%) were purchased from Dae Jung Chem. Co., Korea.

2.2. Methods

2.2.1. Crystallization and phase transformation

A drowning-out approach was applied to crystallize-out the AD crystals and transform them to other polymorphic phases. First, the AD solution was prepared by dissolving 1.65 g of AD in 5 ml of DCM. Then, 5 ml of the AD solution was spontaneously injected into a double-jacket stirred crystallizer (50 ml working volume flask) already loaded with the anti-solvent n-hexane (45 ml). The temperature of the crystallizer was set at −10 °C using the cooling medium of the jacket. After injecting the AD solution, crystallization was induced within minutes, however, the crystal suspension was continuously stirred for 1 h to ensure complete drowning-out of the crystals. Here, the stirring rate of the magnetic bar in the crystallizer remained constant at 450 rpm. The temperature of the suspension was then changed stepwise to a setting value to induce polymorphic phase transformation of the crystals. This stepwise change of the suspension temperature was achieved by suddenly switching from the chilling circulator to the heating circulator set at a target temperature, which allowed the suspension temperature to reach the target value within 10 min. To investigate the effect of the suspension temperature on the phase transformation, the target value was varied from 25 to 55 °C. After reaching the target temperature, 1 ml suspension samples were taken intermittently to monitor the polymorphic transformation.

2.2.2. Analysis

The suspension samples taken from the crystallizer were quickly filtered-out using a vacuum. The solid crystals were then dried and stored in a dessicator until their analysis. The crystal structure was analyzed using powder pattern XRD (Cu-Kα ray (1.54056 Å), M18XHF-SRA, Mac Science, Japan), while the crystal morphology was monitored using an optical video-microscope (Sometech Co., STVMS 305R, Korea). To examine the polymorphism of the crystals, DSC (Q200, TA Instrument, U.S.A.) and TGA (Q5000, TA Instrument, U.S.A.) were used. High pressure liquid chromatography (HPLC, Agilent 1100, Agilent, U.S.A.) was used to measure the solubility of the AD according to various solvent mixtures of DCM and n-hexane and the temperature. For the HPLC analysis, a C18 column was used

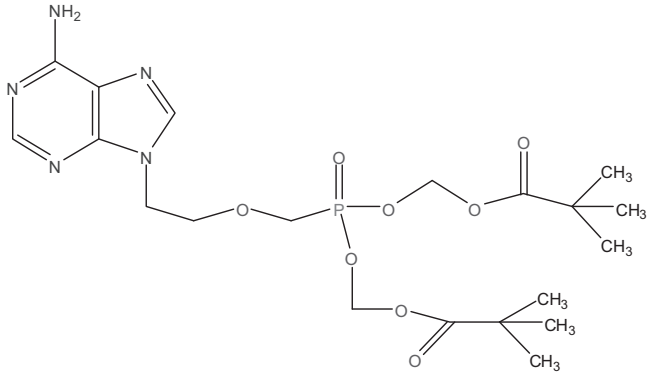

Fig. 1. Molecular structure of adefovir dipivoxil (AD).

and the mobile phase was a water/methanol/acetonitrile mixture (5:4:1, v/v/v) (Fig. 1).

3. Results and discussion

3.1. Polymorph search

The drowning-out crystallization at −10 °C produced adefovir dipivoxil (AD) crystals that were shaped like long sharp needles, as shown in Fig. 2(a). These crystals remained unchanged in their structure and shape when the suspension temperature was kept constant at −10 °C. However, when the suspension temperature was increased stepwise to 40 °C, the crystal shape changed significantly from the initial sharp needle shape to a plate shape after 3.0 h of the stepwise increase (Fig. 2(b)) and then to long rod crystals after 8.0 h (Figs. 2(c and d)). Thus, the distinctive morphological changes of the AD crystals clearly indicated the formation of several polymorphs during the phase transformation in the solution.

Accordingly, the polymorphism of the AD crystals during the phase transformation was examined using power pattern XRD, as shown in Fig. 3. Interestingly, four distinct XRD patterns were identified for the crystals sampled at 1.0, 3.0, 8.0, and 12.0 h, respectively, during the stepwise temperature change. Plus, among these four XRD patterns, the patterns obtained at 1.0 and 8.0 h were found to be distinct from those related to conventional polymorphs. That is, the characteristic peaks of the crystals obtained at 1.0 h (8.0°, 9.5°, 11.2°, 16.4°, 17.6° and 24.5°) and 8 h (6.2°, 6.6°, 6.9°, 7.8°, 12.8°, 21.6°, 22.6°, 23.9°, 25.7°) differed from the characteristic peaks of previously reported polymorphs, as shown in Table 1. However, the XRD patterns for the crystals sampled at 3.0 and 12.0 h were an identical match to those for the conventional form-V and form-I, respectively. Therefore, the new polymorphs formed at 0 and 8 h in the phase transformation were designated as new form-I (NF-I) and new form-II (NF-II), respectively.

It should be mentioned that the XRD patterns for the crystals sampled at 8 h and 12 h appeared quite similar, along with the morphology. However, when magnifying the XRD spectra, several unique characteristic peaks were included in each pattern, as shown in Fig. 3(b). Such similarity in the XRD patterns and crystal shapes between polymorphs has already been frequently observed in the case of conformational polymorphs, where differences arise in both the molecular packing and the molecular conformation in the crystal formation (Teychene et al., 2004, 2006; Teychene and Biscans, 2008).

The polymorphism of the AD crystals was also further examined using DSC and TGA. In the TGA analysis, the crystals sampled at 1.0 h (NF-I crystals) showed a weight loss of about 7.3% at around 60–70 °C, implying a hemi-solvate form including DCM molecules in the crystal lattice (Supporting Material Fig. S-1). Yet, there was no weight loss for the crystals samples at 8 h (NF-II crystals) in a TGA thermal scan up to 120 °C, indicating an ansolvate form of NF-II crystals. Meanwhile, the thermal gravity profiles of the crystals sampled at 3 and 12 h were consistent with ansolvate forms of form-V and form-I, respectively (Supporting Material Fig. S-1). In the DSC analysis, the AD crystals exhibited unique thermal profiles, as shown in Fig. 4. At a 10 °C/min scan speed, the NF-I crystals displayed two endothermic peaks at around 70 and 93 °C. Here, the first peak at 70 °C was due to de-solvation of the crystals, while the second peak at 93 °C resulted from a crystal melt. Interestingly, the melting peak exactly matched the melting temperature of the form-V crystals, indicating that the hemi-solvate NF-I crystals were transformed to ansolvate form-V crystals after de-solvation. Meanwhile, the DSC profiles for the NF-II and form-I crystals only exhibited melting peaks at 97 and 102 °C, respectively.

A thermal scan speed of 10 °C/min, as applied above, is a standard condition for pharmaceutical analyses. Yet, this may be too fast to extract the accurate thermal properties of the polymorphs. Thus, a thermal analysis with a lower scan speed was applied to the AD polymorphs. As a result, when scanned at 1.0 °C/min, the thermal spectrum for the NF-I crystals displayed two endothermic peaks at 93 and 97 °C (A-profile in Fig. 4(b)), corresponding to the melting temperatures of form-V and NF-II crystals, respectively. Furthermore, when lowering the scan speed to 0.1 °C/min, another endothermic peak appeared at 102 °C (B-profile in Fig. 4(b)), corresponding to the melting temperature of form-I crystals. These changes in the thermal spectra according to the DSC scan speed were due to the relative re-crystallization speeds of the melt phase. That is, a scan speed of 10 °C/min for the NF-I crystals was too fast for the melt phase to re-crystallize as NF-II or form-I crystals. Thus, only one melting peak was shown for form-V crystals at 93 °C. However, a slow thermal scan speed of 1 °C/min provided enough time for the melt phase to re-crystallize as NF-II crystals. Meanwhile, the re-crystallization of form-I crystals required a much slower scan speed of 0.1 °C/min. Also, the thermal spectrum at the lowest scan speed revealed that the AD crystals (NF-I) were structurally transformed to form-V → NF-II → form-I, representing the sequential phase stability of the polymorphs. In addition, the appearance of exothermic peaks of re-crystallization right behind the melting peaks also indicated a connection with the monotropic polymorphism.

It should be mentioned that when the NF-II crystals were scanned at 0.1 °C/min, they exhibited two peaks at 97 and 102 °C, corresponding to the melts of NF-II and form-I crystals, respectively. However, when the form-I crystals were scanned, only one melting peak appeared at 102 °C (Supporting Material Fig. S-2). Therefore, the DSC results for the NF-II and form-I crystals provided evidence of the polymorphism between them.

3.2. Solubility of polymorphs

The solubility of each AD polymorph, NF-I, form-V, NF-II, and form-I crystals, was measured with various mixtures of DCM and n-hexane, and at different temperatures, as shown in Fig. 5. To measure the solubility, an excess of NF-I crystals was suspended in a DCM and n-hexane mixture with magnetic agitation. Every 10 min, a 50 μl sample of the solution was taken for an AD concentration analysis using HPLC (Agilent 1100, Agilent, U.S.A.). Using the AD concentration profile over time, the solubilities of the AD polymorphs (NF-I, form-V, NF-II, and form-I crystals) were then determined.

As shown in Fig. 5(a), the solubilities of the AD crystals were highly dependent on the composition of the DCM and n-hexane mixture, being almost insoluble in pure n-hexane (anti-solvent) and highly soluble, as much as 400 mg/ml, in DCM (solvent). In a DCM (10%) and n-hexane (90%) mixture, the solubility was slightly

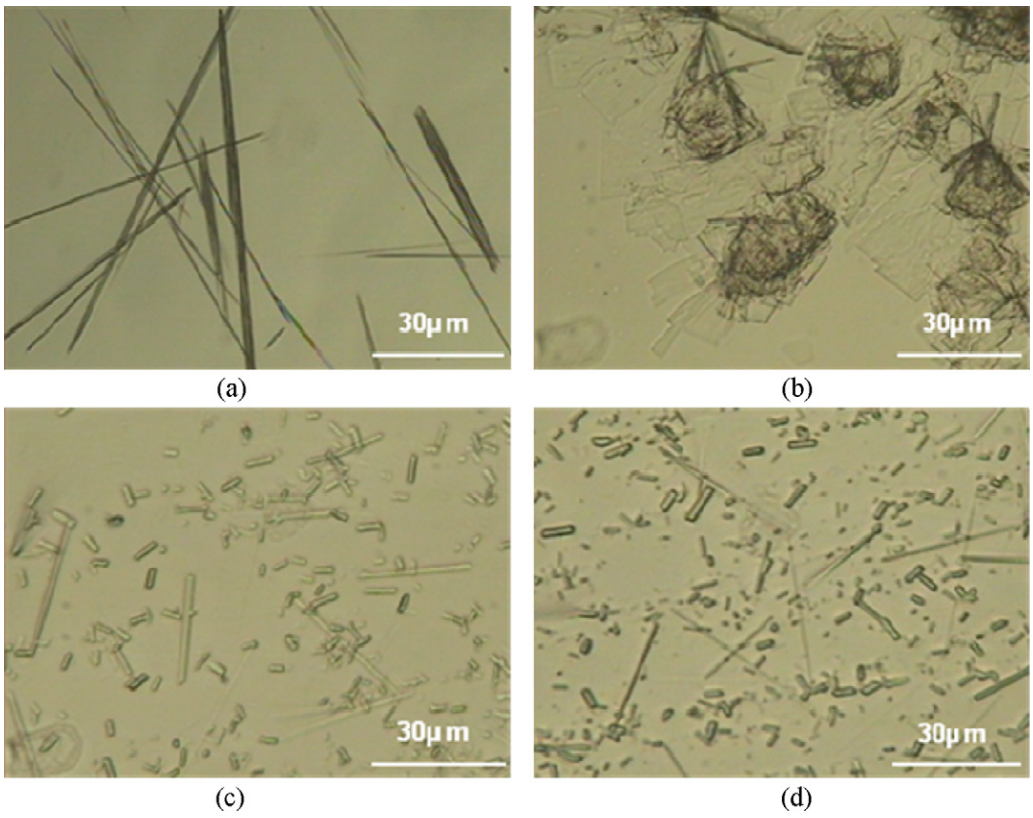

Fig. 2. Morphological change of AD crystals obtained during phase transformation at 40 °C. Crystals were samples at the time of: (a) 1 h, (b) 3 h, (c) 8 h and (d) 12 h in phase transformation.

enhanced when increasing the temperature. Plus, the solubility of the solvate NF-I crystals was always higher than that of the ansolvate crystals of form-V, NF-II, and form-I. Among the ansolvate crystals, the crystals with a higher solubility indicated a relatively metastable phase when compared to the crystals with a lower solubility. In the present study, the solubility of the metastable phase was always higher than that of the stable phase across the entire range of solution mixtures and temperatures, indicating that the ansolvate crystals were monotropic polymorphs. This solubility data can be useful for studying the kinetics of polymorphic transformation.

3.3. Calibration of polymorphic fraction

For a quantitative measurement of the polymorphic transformation, the polymorphic fractions in a pair-wise mixture of crystals among the four polymorphs, NF-I, form-V crystals, were calibrated using the DSC thermal spectra scanned at 10 °C/min, as shown in Fig. 6. Thus, in the case of a mixture of NF-I and form-V crystals, the ratio between the de-solvation peak (NF-I crystals) at 70 °C and the melting peak (form-V crystals) at 93 °C was equivalent to the polymorphic fraction of NF-I crystals in the mixture, as the NF-I crystals were transformed to form-V crystals after the de-solvation (Fig. 6 and Supporting Material Table S-1). Meanwhile, for the three ansolvate crystals, since their respective melting peaks were unique at a high scan speed of 10 °C/min, the peak area for each crystal represented its quantity in the crystal mixture, as shown (Supporting Material Fig. S-3 and Table S-1). These calibrations based on the characteristic peaks of the DSC spectra accurately matched the standard polymorphic fractions of the binary crystal mixtures ($R^2 > 0.99$), and thus could be applied to the kinetics of polymorphic transformation during crystallization.

3.4. Polymorphic transformation

The polymorphic transformation in the solution was measured as shown in Fig. 7, where the drowning-out ratio (volume ratio of DCM to n-hexane) was fixed at 1:9 and the temperature was adjusted from 30 to 55 °C. At a temperature of 35 °C, the NF-I crystals initially generated by the drowning-out crystallization

Table 1
Summary of polymorphs of adefovir dipivoxil (AD).

	Polymorphs	Crystallization method	Solvent	Remarks
Form-I	Anhydrate ($C_{20}H_{32}N_5O_8P$)	Cooling	Acetone + di-n-butyl ether	Gilead Sciences (U.S.A)
Form-II	Dihydrate ($C_{20}H_{32}N_5O_8P{\cdot}2H_2O$)	Drowning-out	Methanol/water	Gilead Sciences (U.S.A)
Form-III	Solvate ($C_{20}H_{32}N_5O_8P{\cdot}CH_3OH$)	Evaporation	Methanol	Gilead Sciences (U.S.A)
Form-IV	Salt form ($C_{20}H_{32}N_5O_8P{\cdot}C_4H_4O_4$)	Cooling	Isopropanol + fumaric acid	Gilead Sciences (U.S.A)
Form-V	Anhydrate ($C_{20}H_{32}N_5O_8P$)	Spray Drying	Ethanol	Tianjin Kinsly Pharm. (China)
Form-VI	Monohydrate ($C_{20}H_{32}N_5O_8P{\cdot}H_2O$)	Evaporation	Methylene chloride + methanol + water vapor	Solmag S.P.A (Italy)
Form-VII	Solvate ($C_{20}H_{32}N_5O_8P{\cdot}C_4H_{10}O$)	Drowning-out	n-Butyl alcohol/hexane	Daehe Chem. (Korea)
Form-VIII	Anhydrate ($C_{20}H_{32}N_5O_8P$)	Drowning-out	AEImBF$_4$(IL)/water	Kyung Hee Univ. (Korea)
Form-IX	Hemihydrate ($C_{20}H_{32}N_5O_8P{\cdot}0.5H_2O$)	Drowning-out	AEImBF$_4$(IL)/water	Kyung Hee Univ. (Korea)

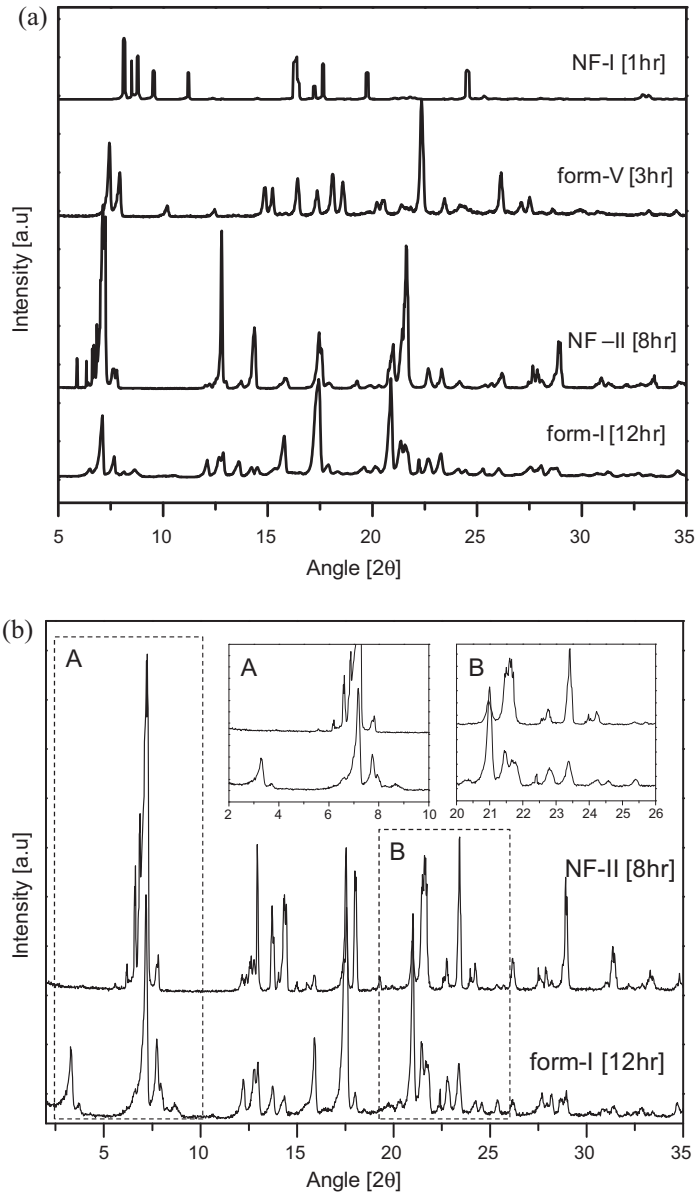

Fig. 3. XRD analysis of AD crystals obtained during phase transformation at 40 °C. (a) XRD patterns of four crystals obtained at 1, 3, 8 and 12 h during phase transformation, and (b) magnified XRD patterns of crystals obtained at 8 and 12 h during phase transformation.

suddenly changed to form-V crystals at around 3 h, followed by a phase transformation to NF-II crystals at 10 h. The NF-II phase then remained unchanged until 16 h and then transformed completely to the form-I phase by 20 h (Fig. 7(a)). When increasing the temperature to 40 °C, the total time for the whole transformation from NF-I phase to the final form-I phase was significantly reduced to 11 h, yet each polymorphic transformation behaved quite differently (Fig. 7(b)). For example, the unchanged period of the NF-II phase was shortened from 6 h to 1 h when increasing the temperature from 35 to 40 °C. In contrast, the unchanged period of the form-V phase was significantly extended to 2 h when increasing temperature to 40 °C. Therefore, these results imply that the phase transformation of each phase was affected differently by the temperature.

The polymorphic transformations among the ansolvate crystals of the form-V, NF-II, and form-I phases were achieved based on a simple reconstructive process in the solution, including the induction of a stable phase and reconstruction of phases by dissolution and growth. However, the transformation of the solvate NF-I phase to the ansolvate form-V phase was different. In this case, the NF-I crystals were first de-solvated to amorphous solids, and then quickly transformed to ansolvate form-V crystals in a reconstructive way (Supporting Material Figs. S-4–S-6). According to the microscopic images (Supporting Material Fig. S-4), the long needle-shaped crystals (NF-I) became irregular tiny particles when de-solvating DCM from the crystal structure. Then, plate-shaped crystals suddenly appeared and quickly replaced all the tiny particles within 10 min. These changes, called pseudo-polymorphic transformation, were confirmed by XRD (Supporting Material Fig. S-5) and DSC (Supporting Material Fig. S-6) analyses. The characteristic XRD peaks of the hemi-solvate NF-I crystals completely disappeared within 30 min and became an amorphous solid pattern. After 10 min, several XRD peaks corresponding to the characteristics of form-V crystals appeared, finally developing into the full pattern of form-V crystals. In addition, the TGA thermal profiles also indicated the shift of the hemi-solvate crystals to ansolvate crystals during the transformation.

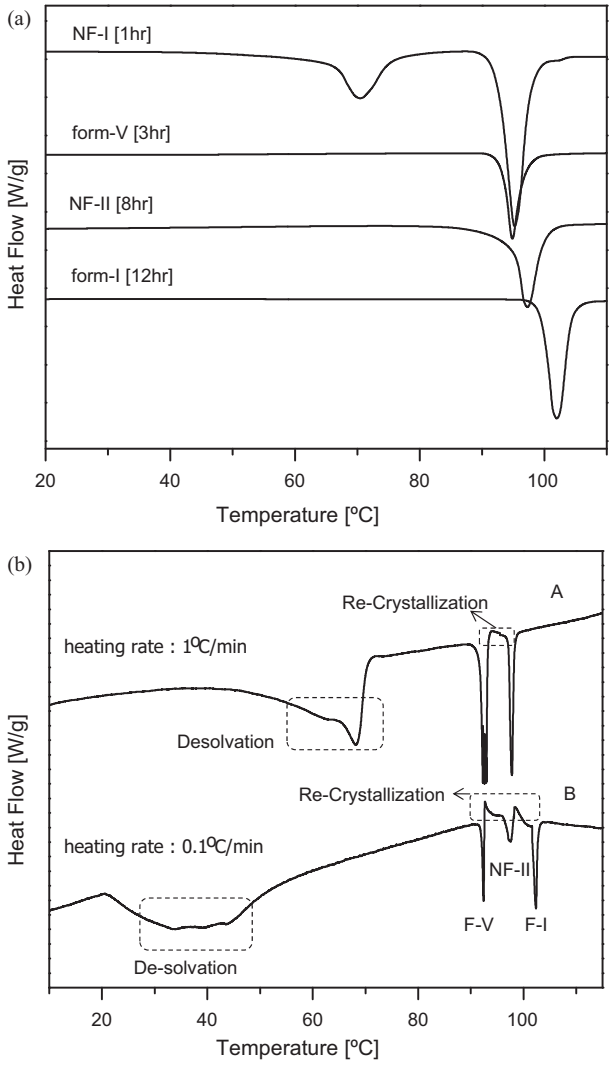

Fig. 4. DSC analysis of AD crystals obtained during phase transformation at 40 °C. (a) Thermal spectra of crystals obtained during phase transformation at 10 °C/min of scan speed. (b) Thermal spectra of crystal obtained at 1 h in phase transformation scanned two different speeds of 1 °C/min and 0.1 °C/min.

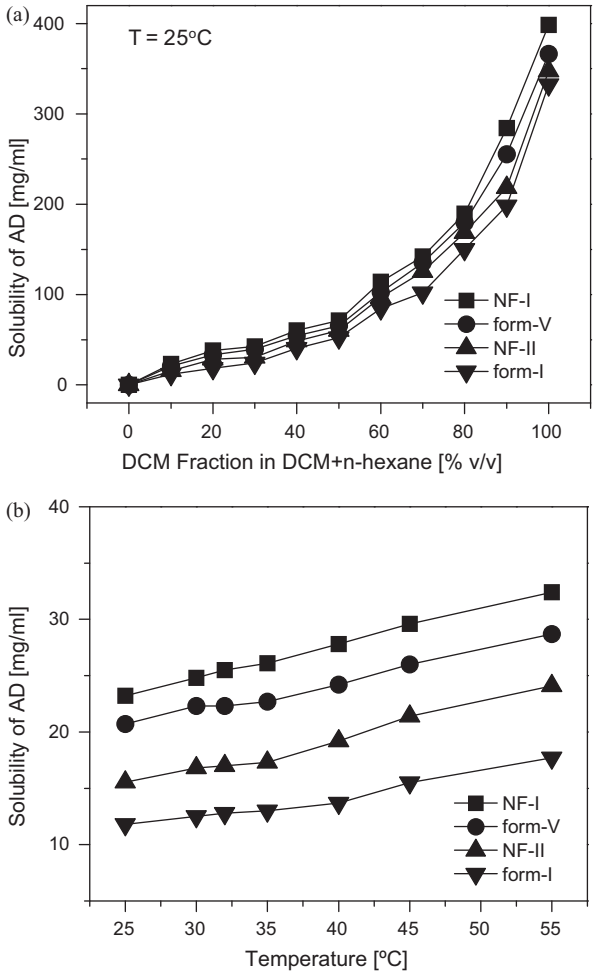

Fig. 5. Solubility of AD polymorphs in dichloromethane-n-hexane mixture varying with: (a) composition of dichloromethane at temperature of 25 °C, and (b) temperature at fixed composition of 10% DCM (v/v%).

In general, the phase transformation process is considered to represent the consecutive steps of the nucleation of stable crystals and the growth of stable crystals based on the simultaneous dissolution of metastable crystals. Thus, for a quantitative investigation of the phase transformation, in the present study, the time period from the initiation of the phase transformation to the first nucleation of stable crystals was counted as the induction time (t_I), and the consecutive time period from the induction point to the completion point, when all the metastable crystals had been converted to stable crystals, was considered as the reconstruction time (t_R). From the profiles of the polymorphic fractions (Fig. 7), the induction and reconstruction times of the polymorphic transformations were then estimated according to the temperature, as shown in Fig. 8. The induction time for form-V was quite high at 13 h with a low temperature of 30 °C, then rapidly reduced to below 3 h when increasing the temperature to 35 °C and only deceased slightly when further increasing the temperature. At a temperature of 25 °C, no polymorphic change occurred until 40 h. Thus, it was assumed that the substantial reduction in the induction time for form-V crystals was due to the significant promotion of the nucleation of form-V crystals with an elevated temperature. Similarly, the induction of form-I crystals was monotonically reduced when increasing the temperature, implying that the temperature facilitated nucleation. In contrast, the nucleation of NF-II crystals was depressed by the temperature, thereby increasing the induction time. Notwithstanding, the reconstruction times for all the

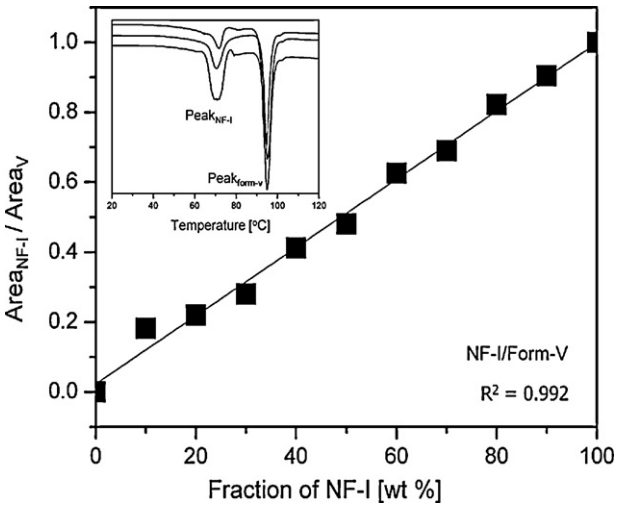

Fig. 6. Calibration of polymorphic fraction in binary mixture of polymorphs, NF-I and form-V crystals (raw data were summarized in Table S-1 of Supporting Material).

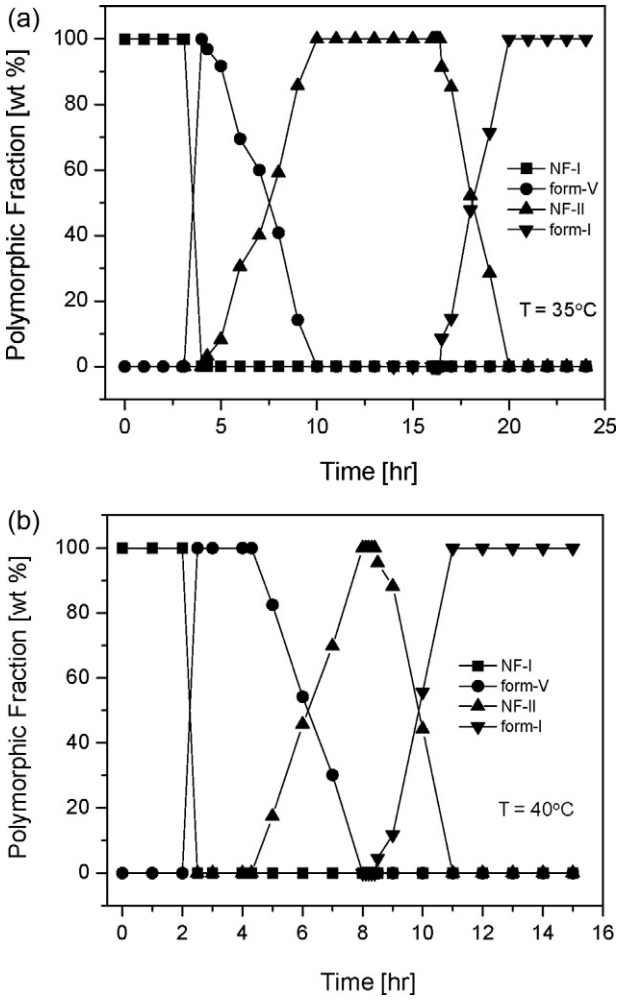

Fig. 7. Profiles of polymorphic fractions during phase transformation at: (a) 35 °C, and (b) 40 °C.

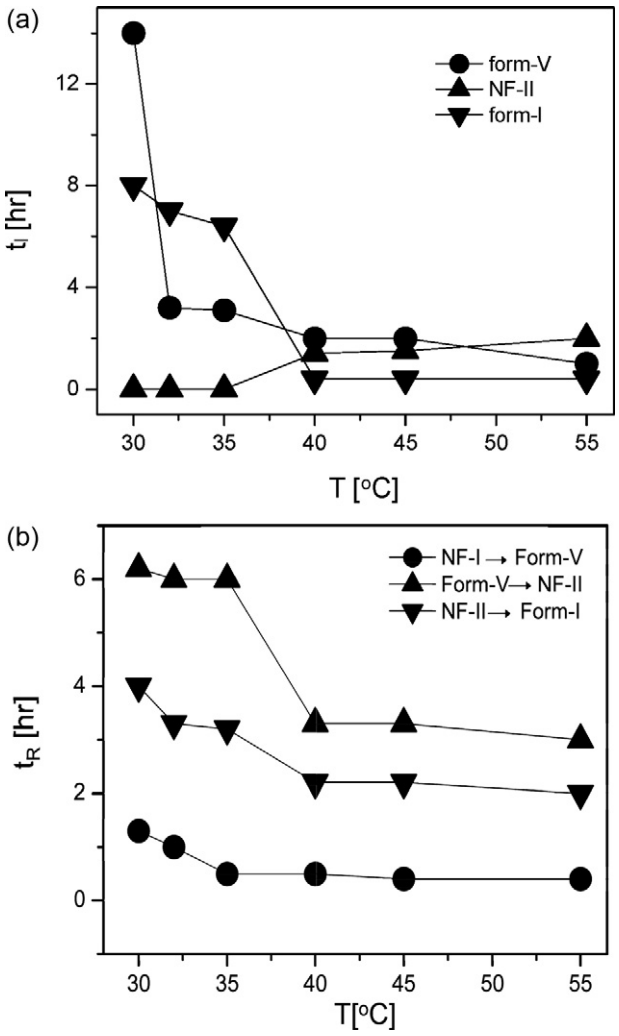

Fig. 8. Dependency of phase transformation rate on temperature. (a) Variation of induction time of polymorphs with temperature, and (b) variation of re-construction time of polymorphs with temperature.

polymorphic transformations always decreased when increasing the temperature, as the growth of stable crystals and dissolution of metastable crystals were both improved (Fig. 8(b)). The dependency of the polymorphic transformation on the temperature will be further discussed in the next section. It should be mentioned that a high transformation temperature above 60 °C resulted in the decomposition of the AD molecules during the phase transformation (Supporting Material Fig. S-7)

3.5. Kinetics of polymorphic transformation

Using Volmer's model, the induction time (t_I), which is inversely proportional to the nucleation rate, can be expressed in terms of the temperature (T) and supersaturation (S) as (Qu et al., 2011).

$$\ln t_I \sim \frac{1}{[T^3 \ln^2 S]} \quad (1)$$

For the induction of the stable phase, the supersaturation is considered as the ratio of the metastable solubility to the stable solubility ($S = C^*_{meta}/C^*_{stable}$). According to Eq. (1), both the temperature and the supersaturation promote induction. Therefore, the influence of the temperature and supersaturation on the induction time was quantitatively estimated, as summarized in Table 2. As shown in Fig. 5, the solubilities of all the polymorphs increased with the temperature. For the transformation to the form-V phase, the supersaturation ($C^*_{NF\text{-}I}/C^*_{form\text{-}V}$) was slightly enhanced when increasing the temperature. Thus, the model equation (Eq. (1)) predicted a decrease in the induction time, which was consistent with the experimental measurement for form-V crystals. However, in the case of NF-II induction, the supersaturation ($C^*_{NF\text{-}I}/C^*_{form\text{-}V}$) was reduced when increasing the temperature. Thus, the induction time was predicted to increase with the temperature, even though the elevated temperature contributed to promote the induction of NF-II crystals. In this case, the induction was predominantly dictated by the supersaturation rather than the temperature. Meanwhile, the form-I induction was mostly dominated by the temperature. As such, the induction time for form-I crystals was reduced when increasing the temperature, although the supersaturation was almost invariant to the temperature (Qu et al., 2011).

The total amount of crystals transformed (m) is related to the mass transfer rate (r) and re-construction time as $m \sim r \cdot t_R$. Plus, under a constant total amount of crystals (m), the reconstruction time is inversely proportional to the mass transfer rate. That is, the reconstruction time is reduced when increasing the mass transfer rate depending on the mass transfer coefficient (k) and concentration difference (ΔC) as $r \sim k \cdot \Delta C$. During the phase transformation, ΔC can be counted as the solubility difference between the metastable and stable phases ($\Delta C = C^*_{meta} - C^*_{stable}$). Based on the film theory, the mass transfer coefficient (k) is related to the diffusivity (D_{AB}) as $k = D_{AB}/\delta$, where δ indicates the mass transfer layer

Table 2
Correlation of induction time in terms of parameters of Volmer's nucleation model.

Form-V				NF-II				Form-I			
T (°C)	S	$[T^3 \ln^2 S]^{-1} \times 10^{-7}$	t_I	T (°C)	S	$[T^3 \ln^2 S]^{-1} \times 10^{-7}$	t_I	T (°C)	S	$[T^3 \ln^2 S]^{-1} \times 10^{-7}$	t_I
30	1.11	32.9	14	30	1.33	4.41	0	30	1.3	5.2	8
32	1.14	20.5	3.2	32	1.32	4.54	0	32	1.3	5.1	7
35	1.15	17.54	3.1	35	1.31	4.76	0	35	1.3	4.9	6.4
40	1.148	16.95	2	40	1.26	6.26	1.4	40	1.4	2.94	0.4
45	1.147	16.39	2	45	1.21	8.33	1.5	45	1.38	2.94	0.4
55	1.145	14.39	1	55	1.19	9.10	2	55	1.36	2.94	0.4

Table 3
Correlation of reconstruction time in terms of parameters of mass transfer rate.

NF-I to form-V				Form-V to NF-II				NF-II to form-I			
T (°C)	ΔC	$[T\Delta C]^{-1} \times 10^{-4}$	t_R	T (°C)	ΔC	$[T\Delta C]^{-1} \times 10^{-4}$	t_R	T (°C)	ΔC	$[T\Delta C]^{-1} \times 10^{-4}$	t_R
30	2.5	13.2	1.3	30	5	6.6	6.2	30	4	8.24	4
32	3	10.92	1	32	5	6.55	6	32	4.2	7.8	3.3
35	3.4	9.64	0.5	35	5	6.49	6	35	4.3	7.5	3.2
40	3.6	8.87	0.5	40	5	6.39	3.3	40	5.5	5.81	2.2
45	3.6	8.73	0.4	45	5	6.29	3.3	45	5.9	5.33	2.2
55	3.7	8.24	0.4	55	5	6.09	3	55	6	5.08	2

thickness. Then, using the Stokes–Einstein equation, the diffusivity is expressed as a function of the temperature as $D_{AB} = kT/6\pi\gamma_0\mu$ (McCabe et al., 2005). Therefore, the reconstruction time can be described in terms of the temperature and solubility difference of the metastable and stable phases as:

$$t_R \sim \frac{1}{r} \sim 1[T(C^*_{meta} - C^*_{stable})] \quad (2)$$

Thus, using the solubility data for the polymorphs (Fig. 5), the dependency of the reconstruction time on the temperature was predicted as summarized in Table 3. For the reconstruction of NF-I crystals to form-V crystals and NF-II crystals to form-I crystals, the mass transfer coefficient and solubility difference were both increased when increasing the temperature, thereby facilitating the reconstruction process. Meanwhile, for the reconstruction of form-V crystals to NF-II crystals, the solubility difference was almost independent of the temperature. Thus, the reduction of the reconstruction time was mostly attributed to the promoted mass transfer coefficient when increasing the temperature.

The kinetics of the phase transformation, i.e., the induction and reconstruction times, were plotted as functions of $T^3 \ln^2 S$ and $T\Delta C$,

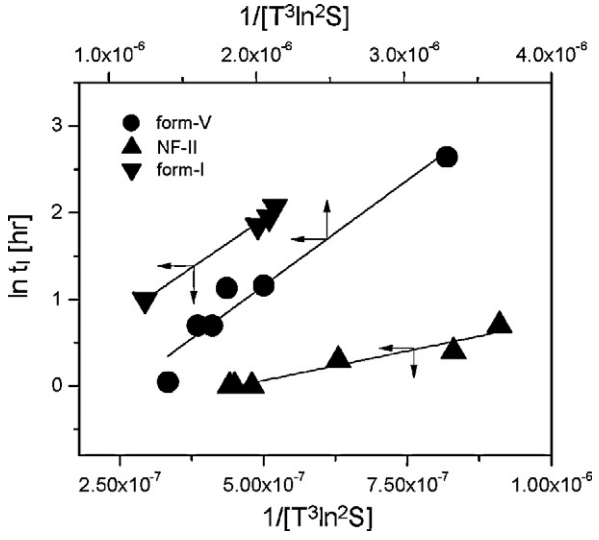

Fig. 9. Kinetic correlation of induction time of polymorphs in phase transformation based on Volmer's nucleation model.

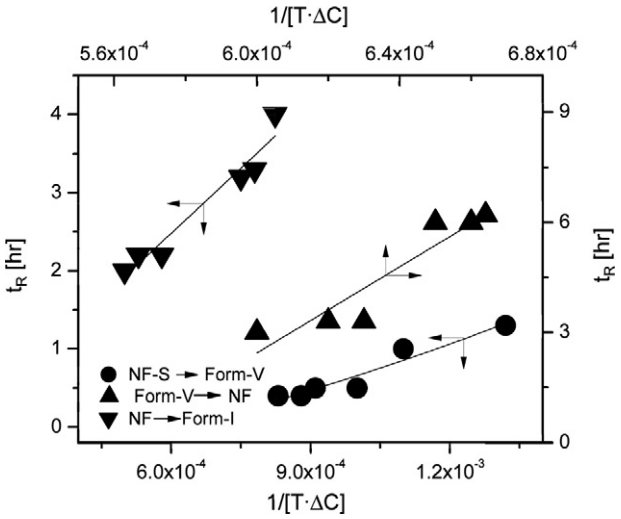

Fig. 10. Kinetic correlation of re-construction time of polymorphs in phase transformation based on film theory mass transfer rate.

respectively, as shown in Fig. 9. The induction of NF-II crystals was much faster than that of any other polymorph, yet less sensitive to the parameter $(1/[T^3 \ln^2 S])$ during the phase transformation Fig. 9. In addition, the reconstruction time for the phase transformation of form-V crystals to NF-II crystals was most dependent on the mass transfer rate $[T\Delta C]$, although the mass transfer rate was least dependent on the temperature Fig. 10. Therefore, these results confirmed that the induction and reconstruction times were linearly aligned on the plot of $1/[T^3 \ln^2 S]$ and $1/[T\Delta C]$, respectively, indicating that the kinetic variation of the phase transformation with the temperature was mainly due to the nucleation and mass transfer rates depending on the temperature.

4. Conclusion

This study demonstrated the possibility of identifying new polymorphs of AD during the phase transformation in a solution. A new solvate polymorph, NF-I, was produced by drowning-out crystallization when using DCM as the solvent and n-hexane as the anti-solvent. Since the solvate crystals were stable at a low temperature below 25 °C, no phase transformation was induced in the

solution. However, when increasing the temperature above 30 °C, phase transformation occurred to change the solvate crystals to stable ansolvate crystals via form-V → NF-II → form-I.

The AD crystal polymorphs were determined using DSC, TGA and XRD analyses and confirmed by solubility measurements. According to the TGA analysis, the initial solvate crystals were hemi-solvates, whereas the form-V, NF-II, and form-I crystals that occurred during the phase transformation were all ansolvates. In the DSC analysis, the solvate NF-I crystals changed to form-V crystals via desolvation at around 70 °C. The form-V crystals were then recrystallized to NF-II crystals at around 93 °C and changed to form-I crystals at around 97 °C. The form-I crystals melted at 103 °C, which was consistent with the melting point reported in a previous study.

The kinetics of the phase transformation varied significantly with the temperature, as the solubility of the polymorphs, the driving force for induction and reconstruction, depended on the temperature. The induction time for stable crystals was dictated by the temperature and supersaturation ($\ln t_l \sim 1/[T^3 \ln^2 S]$). As such, increasing the temperature contributed to a reduced induction time for stable crystals. However, the supersaturation ($S = C^*_{meta}/C^*_{stable}$) exhibited a case by case dependency on the temperature. Therefore, in the polymorphic transformations from NF-I to form-V and from NF-II to form-I, the supersaturation increased with the temperature. However, in the polymorphic transformation from form-V to NF-II, the supersaturation was reduced with the temperature, resulting in an increased induction time. Notwithstanding, the reconstruction time was monotonically reduced when increasing the temperature due to the promotion of the mass transfer rate. These kinetics of the phase transformation, described in terms of the induction and reconstruction times, were consistent with the experimental results.

Acknowledgement

This study was financially supported by the NRF Research Fund (Korea, 2010-0017993).

Appendix A. Supplementary data

Supplementary data associated with this article can be found, in the online version, at doi:10.1016/j.ijpharm.2011.10.049.

References

An, J.H., Kim, J.M., Chang, S.M., Kim, W.S., 2010. Application of ionic liquid to polymorphic design of pharmaceutical ingredients. Cryst. Growth Des. 10, 3044–3050.
Bernstein, J., 2002. Polymorphism in Molecular Crystal. Clarendon Press, Oxford.
Chemburkar, S.R., Bauer, J., Deming, K., Spiwek, H., Patel, K., Morris, J., Henry, R., Spanton, S., Dziki, W., Porter, W., Quick, J., Bauer, P., Donaubauer, J., Narayanan, B.A., Soldani, M., Riley, D., McFarland, K., 2000. Dealing with the impact of ritonavir polymorphs on the late stages of bulk drug process development. Org. Process Res. Dev. 4, 413–417.
Davey, R.J., Cardew, P.T., 1986. Rate controlling processes in solvent-mediated phase transformations. J. Cryst. Growth 79, 648–653.
Doremus, R.H., 1985. Rates of Phase Transformations. Academic Press, New York.
Gu, C.H., Young Jr, V., Grant, D.J.W., 2001. Polymorph screening: influence of solvents on the rate of solvent-mediated polymorphic transformation. J. Pharm. Sci. 90, 1878–1890.
Hilfiker, R., 2006. Polymorphism: in the Pharmaceutical Industry. Wiley-VCH, Weinheim.
Kiang, Y.H., Huq, A., Stephens, P.W., Xu, W., 2003. Structure determination of enalapril maleate form II from high-resolution X-ray powder diffraction data. J. Pharm. Sci. 92, 1844–1853.
Kitamura, M., Hara, T., 2007. Dependence of polymorphism on molecular structure of BPT esters. Cryst. Growth Des. 7, 1575–1579.
Kitamura, M., Hara, T., Takimoto-Kamimura, M., 2006. Solvent effect on polymorphism in crystallization of BPT propyl ester. Cryst. Growth Des. 6, 1945–1950.
Kurotani, M., Hirasawa, I., 2008. Polymorph control of sulfamerazine by ultrasonic irradiation. J. Cryst. Growth 310, 4576–4580.
Liang, K., White, G., Wikinson, D., 2004. An examination into the effect of stirrer material and agitation rate on the nucleation of L-glutamic acid batch crystallized from supersaturated aqueous. Cryst. Growth Des. 4, 1039–1044.
Lu, J., Rohani, S., 2009. Polymorphic crystallization and transformation of the antiviral/HIV drug stavudine. Org. Process Res. Dev. 13, 1262–1268.
Martinez-Oharriz, M.C., Martin, C., Goni, M.M., Rodríguez-Espinosa, C., Tros De Ilarduya-Apaolaza, M.C., Sánchez, M., 1994. Polymorphism of diflunisal: isolation and solid-state characteristics of a new crystal form. J. Pharm. Sci. 82, 174–177.
Maruyama, S., Ooshima, H., 2000. Crystallization behavior of taltirelin polymorphs in a mixture of water and methanol. J. Cryst. Growth 212, 239–245.
McCabe, W.L., Smith, J.C., Harriott, P., 2005. Unit Operations of Chemical Engineering. Mc Graw Hill.
Mirmehrabi, M., Rohani, S., 2006. Polymorphic behavior and crystal habit of an antiviral/HIV drug: stavudine. Cryst. Growth Des. 6, 141–149.
Mirza, S., Miroshnyk, I., Heinarnaki, J., Christiansen, L., Karjalainen, M., Yliruusi, J., 2003. Influence of solvents on the variety of crystalline forms of erythromycin. AAPS Pharm. Sci. 5, 39–47.
Pereira, B.G., Fonte-Boa, F.D., Resende, J.A.C.L., Pinheiro, C.B., Fernandes, N.G., Yoshida, M.I., Vianna-Soares, C.D., 2007. Pseudopolymorphs and intrinsic dissolution of nevirapine. Cryst. Growth Des. 7, 2016–2023.
Purohit, R., Venugopalan, P., 2009. Polymorphism: an overview. Resonance 14, 882–893.
Qu, H., Kultanen, M.L., Rantanen, J., Kallas, J., 2006. Solvent-mediated phase transformation kinetics of an anhydrate/hydrate system. Cryst. Growth Des. 6, 2053–2060.
Qu, H., Kultanen, M.L., Rantanen, J., Kallas, J., 2007. Additive effects on the solvent-mediated anhydrate/hydrate phase transformation in a mixed solvent. Cryst. Growth Des. 7, 724–729.
Qu, H., Munk, T., Cornett, C., Wu, J.X., Botker, J.P., Christensen, L.P., Rantanen, J., Tian, F., 2011. Influence of temperature on solvent-mediated anhydrateto-hydrate transformation kinetics. Pharm. Res. 28, 364–373.
Sarma, B., Chen, J., His, H.Y., Myerson, A.S., 2011. Solid form of pharmaceuticals: polymorphs, salts and cocrystals. Korean J. Chem. Eng. 28, 315–322.
Sato, K., Suzuki, K., Okada, M., Garti, N., 1985. Solvent effects on kinetic of solution-mediated transition of stearic acid polymorphs. J. Cryst. Growth 72, 699–704.
Smith, J.R., Xu, W., Raftery, D., 2006. Analysis of conformational polymorphism in pharmaceutical Solids using solid-state NMR and electronic structure calculations. J. Phys. Chem. 110, 7766–7776.
Teychene, S., Biscans, B., 2008. Nucleation kinetics of polymorphs: induction period and interfacial energy measurements. Cryst. Growth Des. 8, 1133–1139.
Teychene, S., Autret, J.M., Biscans, B., 2004. Crystallization of eflucimibe drug in a solvent mixture: effects of process conditions on polymorphism. Cryst. Growth Des. 4, 971–977.
Teychene, S., Autret, J.M., Biscans, B., 2006. Determination of solubility profiles of eflucimibe polymorphs: experimental and modeling. J. Pharm. Sci. 95, 871–882.